

A Thesis Presented to
The Faculty of Alfred University

The Exploration of Water Condensation as a
Dependable Provider of an Improved Water Source

by

Luke S. Perry

In Partial Fulfillment of
The Requirements for
The Alfred University Honors Program

May 5, 2017

Under the Supervision of:

Chair: Dr. Joseph D. Kirtland Assistant Professor of Physics, Physics and Astronomy
Department, Alfred University

Committee Members:

Dr. John D'Angelo Associate Professor of Chemistry, Chemistry Department, Alfred
University

Dr. Roger J. Loucks Professor of Physics, Physics and Astronomy Department, Alfred
University

Introduction

Access to basic water needs within a region is a necessity for human habitation. Potable freshwater is the most beneficial to personal health. It can also be used for a variety of other needs in society including, but not limited to industrial and agricultural uses. As such, scarcity of freshwater can not only have an impact on health of individuals, but also on the socio-economic status of a country. Water scarcity worsens any problems already existing, and imposes extra strain on different governmental and private agencies, limiting a country's ability to solve issues connected with water scarcity.* Therefore, to combat the problems of water scarcity, one cannot always rely on larger institutions' abilities to solve issues without proper countermeasures in place beforehand. Instead, other solutions that may be implemented on a smaller scale must be explored and developed to alleviate any extra burdens placed on existing systems for preventative and corrective actions. The purpose of this paper is to explore the energy requirements and viability of providing potable water by condensing water from ambient air.

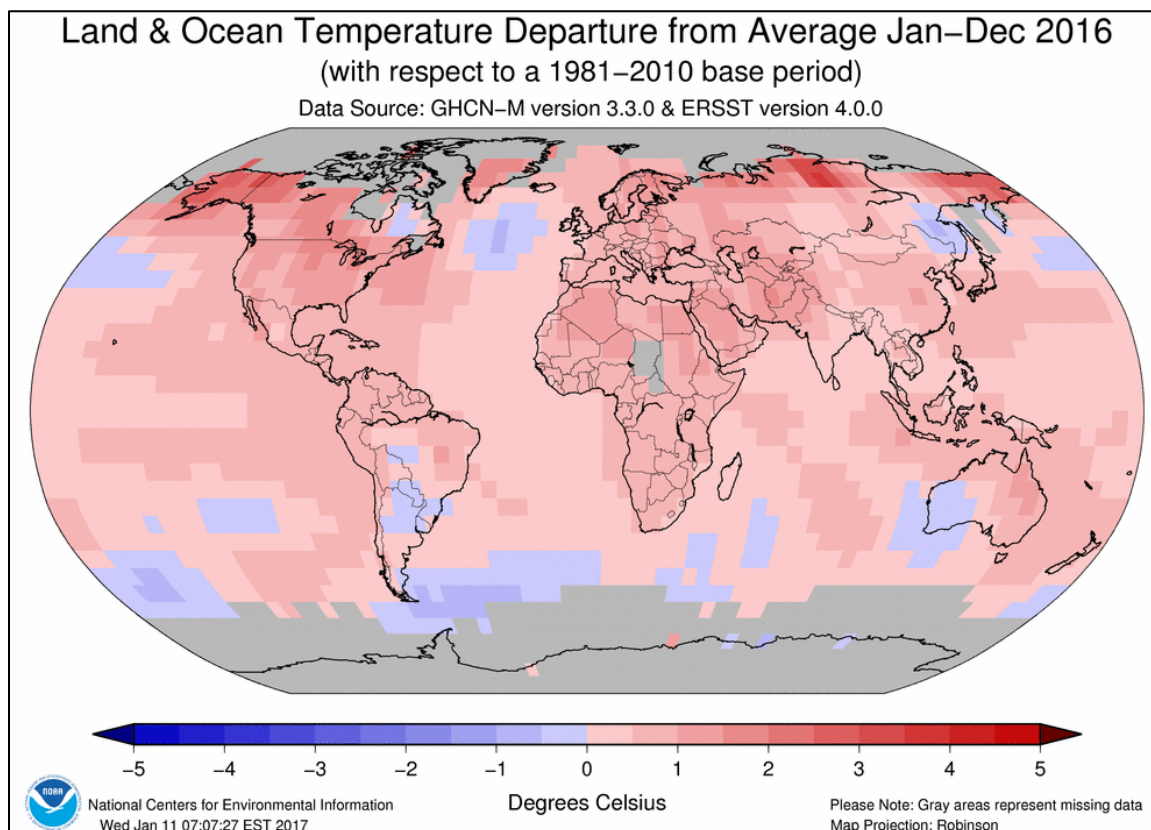


Figure 0.1 The average temperatures the National Centers for Environmental Information is comparing against are 1981-2001 values for each region.[†]

With a growing global population and a globally changing climate, water scarcity is expected to worsen in many countries that have had a history of having a plentiful supply of water while also growing more severe in areas that already had a previous record of an insufficient water supply. As the planet approaches a 2°C increase from historic averages, the average number of people

* *J. Schewe, et. Al.*

[†] "Global Climate Report - Annual 2016."

living in water scarcity could increase anywhere from 40% to 100%.^{*} This is due to an overall increase of population as well as increased extreme environmental conditions. Some areas around the globe have already started to feel these effects, especially in Central America and Central Africa.[†]

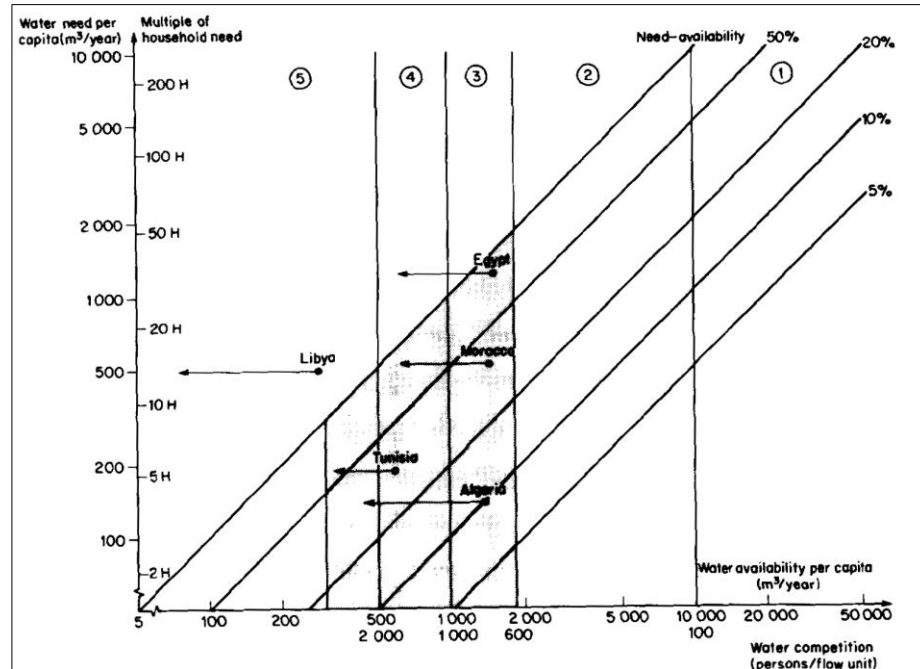


Figure 0.2 This graph was created in 1989 to show how different regions of the world experience water scarcity or are at risk of water scarcity. Regions 3, 4, and 5 experience levels of water scarcity, region numbers increasing with severity of water scarcity.[‡]

One must first develop an understanding of how and in what ways water resources impact different areas of the globe to develop engineered structures that will address current and future problems involving water resources. Water scarcity has become an increasing concern among those studying how it is managed. An important step to addressing water scarcity is determining how much water each person within a society consumes. The amount of water overall varies depending on what the needs of the society are and the local environment. The more developed a nation is, the greater are its water needs per person.[§] This is in large part due to the demands of hydropower, thermonuclear power plants and agriculture.^{**} However, Falkenmark et al. estimated that for a society to have only slight problems exacerbated or created by water scarcity, there should be on the order of one million m³ per 2,000 persons per year in any given region. Below this, the environment begins to become at risk for water stress, which in turn can lead to the development of water scarcity issues.

While industrialized nations often consume more water, there is a large drive for the efficient use of resources in more industrialized nations, especially those that have a history of water scarcity problems. This can alleviate some of the stress on water resource management.

* J. Schewe, et. Al.

† J. Schewe, et. Al.

‡ Falkenmark, Malin, Jan Lundqvist, and Carl Widstrand.

§ Falkenmark, Malin, Jan Lundqvist, and Carl Widstrand.

** J. Schewe, et. Al.

Despite these efforts, global water demands are largely increasing. There are some areas that are consuming less water, but the number of people experiencing water scarcity is increasing globally.*

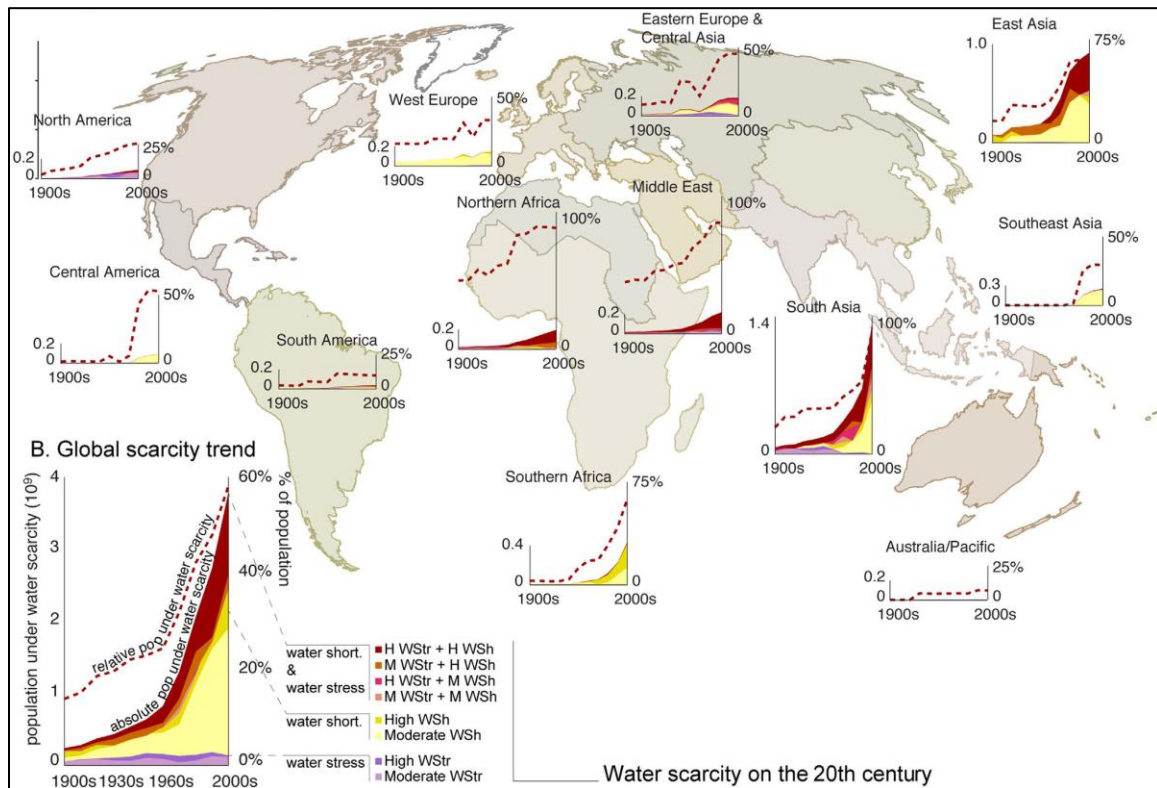


Figure 0.3 Water scarcity around the world in the 20th century. Most regions around the world have experienced a trend of increased water scarcity; however, East Asia and South Asia have improved dramatically in the last 40 years.†

Another problem is that even if a country moves toward more efficient ways of using water, this often requires larger infrastructure and a capable administration, which can be fiscally costly.‡ As such, this limits the availability of such methods to regions of the world that are relatively stable and prosper economically. In 2014, countries were asked to report on the status of water resources, both sanitation and access to improved drinking sources. Of 93 countries that reported on national policies for drinking water, 30% responded that plans were being fully implemented. However, this number is inflated as only 80% of responding countries indicated that a national policy was in place and had been publicly announced. Only a total of 22 countries are fully implementing national policies on drinking water, or less than 25% of the total 93 reporting. The lack of implementation by the remaining 52 countries that have public, national policies on drinking water is attributed to mismanagement or lack of financial resources, or inadequate or non-functioning administrative oversight. 80% of reporting countries stated that financial resources were not sufficient to fully implement policy, while 77% indicated that tariffs were not adequate to cover the costs of operation and maintenance. In terms of manpower, only

* Kummu, et. Al.

† Kummu, et. Al.

‡ Falkenmark, and Widstrand.

one third of reporting countries indicated that they had agencies to address hiring and manpower allocation for water resources and sanitation even in the face of acknowledging staffing issues in water management and regulation. These contributing factors are most associated with developing countries, which are at the highest risks for lack of proper sanitary conditions to begin with as well as having water sources which may be already, or could easily become, contaminated*.

The most common contaminant in water sources is fecal matter, which is a major contributor to the development of diarrheal diseases. The introduction of improved water sources to over 2.3 billion people worldwide has resulted in a decrease of infant mortality from 1.5 million in 1990 to just over 600,000 in 2012.[†] Due to many water sources being groundwater sources or local bodies of water, whether still or moving, the introduction of proper sanitation facilities is most effective in preventing fecal materials from gathering in water sources. However, this can become costly, especially in areas that do not have proper infrastructure such as properly functioning sewage systems. Therefore, water can also be treated using a combination of methods, including suspended solid filtering, introduction of disinfecting chemicals such as chlorine, and other methods not commonly used.[‡] Not only are such water purification endeavors costly to establish, but they can become financially burdensome on the administration overseeing such programs. Standard methods of water purification often have a facility that is operated and maintained by a staff at all times. And although new advances of monitoring techniques have been recently explored such as using cellular phones and mobile devices as part of facility communications and monitoring, the implementation of a widespread program that does not directly use professionally trained individuals to physically staff a water treatment compound has not been accomplished. However, it has become apparent that the costs of operating a water treatment facility can be reduced by using remote monitoring equipment.[§]

With such revolutionary ideas succeeding at small scales in implementation, it is useful then to pursue alternative paths to freshwater collection. As early as 1989, it was recognized that in regions around the globe, the needs of a growing population would rise above the water resources available. Within a given region, there is only so much naturally occurring rainfall per year. If the needs of a given population rise above that region's water production per year, then man-made landscape dessication may occur, temporarily or permanently lowering the water tables for that region. To combat this process, more water must be imported into the water cycle. This can occur by directly importing freshwater into the local environment from a foreign source or using desalination to purify saltwater into freshwater.** The process of desalination is costly, but can ultimately satisfy a region's water needs if resources are available to do so. Importing water from another region is often less costly; however, this is only a temporary solution as the population, and, therefore the water needs in the exporting region could easily change, resulting in both regions experiencing water scarcity. Both solutions often require large amounts of infrastructure and administration, which may not always be available. To address the needs of people who are in less developed parts of the world, who may not have access to or whose

* *GLAAS 2014 Report* Within this report, data is self-reported. Therefore, some of the information may have been skewed, unreported or incomplete for several countries. However, this is the most complete, globally comprehensive information available to date.

† *GLAAS 2014 Report*

‡ *World Health Organization. Guidelines for drinking-water quality.*

§ *Kumpel et. Al.*

** *Falkenmark, Malin, Jan Lundqvist, and Carl Widstrand.*

country may not have access to the resources available to classically address water scarcity, one must pursue alternative solutions while simultaneously improving current ones.

One of the ways which has been recently explored is the development of inexpensive condensers to provide water for small communities in regions that are most affected by water scarcity. Condensation often requires a large amount of energy to lower the temperature of ambient air to below the current dew point temperature. However, clever techniques can be implemented to allow either the dew point temperature of air to be raised or to lower the temperature of the air with little energy required. The strategies for producing the energy that is necessary to operate any equipment used can either implement standard techniques where the environment supplies direct mechanical energy, or use recent technologies that harness natural resources to generate electricity such as wind turbines or solar panels. By exploring the use of new technologies as well as concretely developed physical theories, new solutions or more efficient ways of using previous solutions may be found.

In this paper, elementary fluid mechanics, thermodynamics and statistical mechanics are utilized to explore the opportunity that a pressure difference may offer to potable water production. The framework presented in this paper is not to be followed as a concrete set of directions to solve problems, but rather provide an application of physics to a proposed solution to a societal stressor. The mathematics that is laid out in this paper is arranged in such a way as to be straightforward; however, a background in differential equations, thermal physics, fluid mechanics, and meteorological sciences is important to understanding the foundations on which arguments are built.

Section 1 describes the methodology behind the study, including the derivation of the equations used and the discussion of the computer software. Section 2 includes the graphical data produced from the programs used. Section 3 presents the major findings of this study. Section 4 discusses how the results from this research are applicable and how they can be interpreted.

Section 1. Methods

A system composed of a long tube constricting into a smaller tube, then suddenly dilating to the original size was used to analyze how efficiently water vapor could be extracted from air using a pressure gradient. The system was designed to produce a decrease in pressure across the initial channel until a dilation near the exit. Assuming air behaves as an incompressible fluid, the slope decreases the cross-sectional area the fluid is moving through, which forces air to increased velocities, and subsequently to a higher pressure for the same velocity by the kinetic theory of gases. In this case, the pressure is not reduced as steeply across the length of the system.

Elmer finite element analysis software was used to determine how effective two different geometry parameters were: tube length and slope of convergence by solving the Navier-Stokes Equation, Eq. 1 and Eq. 2.

Four systems were analyzed using computational software due to the fact that analytic solutions to the Navier-Stokes Equation cannot be found in all instances. This is due to the nonlinearity of the equation. Dirichlet boundary conditions were used to hold both the entrance and the exit at a constant velocity, constant turbulent kinetic energy, and constant kinetic energy dissipation rate. All other walls were considered no-slip and had a fixed boundary layer thickness for each system. These values were calculated using standard assumptions of the k-epsilon turbulence model, and previous experimentally determined relationships.

$$(1) \quad \rho \frac{D}{Dt} \mathbf{v} = -\nabla p + \mu \nabla^2 \mathbf{v} + \rho \mathbf{g}^*$$

$$(2) \quad \frac{Dv_i}{Dt} = \frac{\partial v_i}{\partial t} + v_x \frac{\partial v_i}{\partial x} + v_y \frac{\partial v_i}{\partial y} + v_z \frac{\partial v_i}{\partial z} \dagger$$

	<u>Center Tube Diameter (mm)</u>
System A	8
System B	6
System C	4
System D	2

Table 1.1 The entrance and exit chambers are 10 mm in diameter.

Each system was designed and created using Gmsh, a multi-dimensional finite element grid generator. Because of the axial symmetry, each system was created as a two-dimensional grid, rather than a three-dimensional system. While there may be small differences in pressure distributions between neighboring grid cells, overall the pressure differences across each cross-sectional area should be minimal.

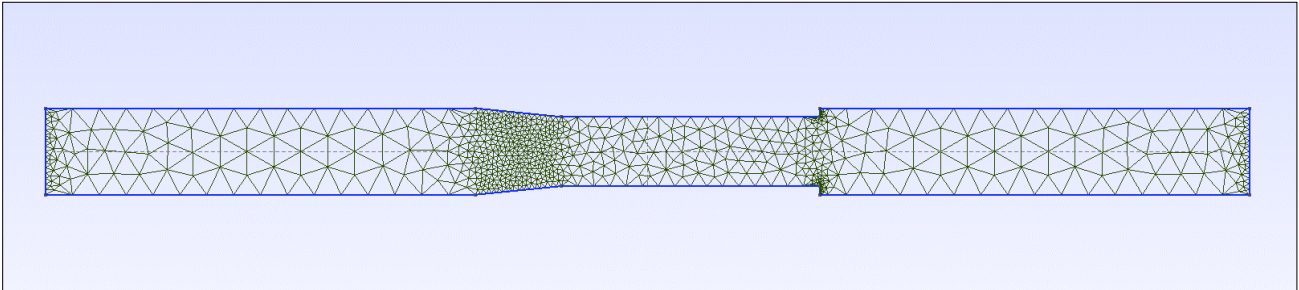


Figure 1.1 An example of how a two-dimensional grid is generated on the system. At points where there could be interesting behavior the mesh partitions into finer elements.

The pressure difference used in the simulations was determined by using average relative humidity values, temperature and surface pressure for a temperate climate during the Spring and Fall seasons. This was done as it represents a moderate climate, as opposed to choosing an arid climate in which the humidity, surface pressure, and temperature are much higher than in other environments.[‡] The opposite can be said of colder climates. Because any technique of providing water should be tested in a variety of climates, a temperate environment was chosen to best represent a middle-ground between extremes. Arid climates have higher temperatures, and therefore may pose a challenge; however, the humidity in such climates is higher as well. In

* Bolded quantities represent vectors.

† v_i represents the i^{th} component of the velocity, where i is x , y , or z . Eq. 1 therefore represents 3 equations, one for each component.

‡ While it is intuitive that in arid regions humidity would be lower, it is in fact the opposite. This is due to higher temperatures, which causes water to move into the vapor state rather than stay in the liquid state. Because temperatures rarely fluctuate low enough for the relative humidity to reach above 100%, the water table is much lower, making the ground dryer, and making it seem as though there should be less water in the air.

contrast, tropical climates such as rainforests have higher humidity, but highly fluctuating temperatures, averaging to be slightly higher than temperate environments. Therefore, by choosing a temperate climate, the system can be tested, but its use not defined by any environment that is characterized by either humidity or temperature.

The average relative humidity fluctuates between an average of 40%-65%.^{*} Therefore, 50% relative humidity was used, not only due to the average within a temperate region, but also due to the global average humidity showing a decreasing trend over the past twenty years.[†] A temperature of 18.3°C was used as it was the average of the average highs in temperature across September to November.[‡] The dew point temperature was calculated using Eq. 3, published by Dr. Mark G. Lawrence, in which T_d is dew point temperature, T is current temperature, and RH is current relative humidity.[§] While this equation is an approximation, it is especially accurate around 15°C, which is near the operating temperature.

$$(3) \quad T_d \approx T - \left(\frac{100-RH}{5} \right)$$

After calculating Equation 3, one can use Eq. 4, the relationship between the heat capacity per volume of air to the temperature and pressure of air to find the needed pressure difference. C_v is specific heat at constant volume, V is volume, f is degrees of freedom per molecule, and P is pressure.^{**}

$$(4) \quad T \frac{C_v}{V} = \frac{f}{2} P$$

If one assumes air to be ideal and diatomic, then $f=5$. If we also assume that for small temperature changes, such as those that air undergoes with precipitation, the specific heat capacity should remain constant with a difference in temperature. Under these assumptions, one can find the pressure change needed for a system to reach dew point temperature by using Eq. 3 and 4, giving Eq. 5, where ΔP is the difference between the final surface pressure and the initial surface pressure.^{††}

$$(5) \quad 2C_v \left(\frac{100-RH}{25} \right) = \Delta P$$

Globally, and across the United States, surface pressures oscillate between 99 kPa and 101 kPa.^{‡‡} Using the specific heat of air, taken to be 717 J/(kg·K), one finds a necessary pressure

^{*} "Comparative Climatic Data." National Climatic Data Center.

[†] "2013 State of the Climate: Humidity." The specific humidity has been increasing during the same period due to the melting of glaciers, but due to increasing global temperatures, it has not produced an increase in relative humidity.

[‡] "Climate United States." In calculating the average, the number of days within a month was accounted for, October being the longest of the three months. The data used is averaged from 1961-1990. Therefore, it may be slightly lower than what is experienced today.

[§] Lawrence, Mark G.

^{**} Schroeder, Daniel V.

^{††} The change in sign of this equation is due to the difference between enacting a change in a system that is the same as a temperature change rather than equilibrating the system so that it does not change, which is the original expression without the change of sign.

^{‡‡} "North American Surface Analyses." Weather Prediction Center.

difference of 1872 Pa.* The goal of this calculation is to obtain a pressure at which the water vapor would be saturated in a parcel of air. If a near-constant pressure can be maintained across an open system, this could be utilized to condense water if a larger pressure difference is added across the system. Of course, a constant pressure across a system of moving air would be ideal, but is not possible in an open system with an incompressible moving fluid.†

The maximum energy efficiency of producing such a pressure difference is governed by Carnot's Theorem. The maximum efficiency of any system creating the same pressure difference can be determined by using this theorem, conservation of energy, and the ideal gas law. This gives Eq. 6, e being the efficiency of the system. Efficiency has a value that ranges from 0 to 1. Values of 1 represent the complete conversion of heat energy into work, which through Carnot's result is physically impossible.‡ Eq. 6 places a lower limit on the amount of energy required to produce a pressure difference on any system.

$$(6) \quad e = 1 - \frac{P}{P + \Delta P}$$

Until now, this paper has only addressed the requirements to reach the dew point temperature, but not discussed energy requirements to condense water afterwards. After a given parcel of air is at dew point conditions, latent heat energy must be removed for it to condense. This is governed by Eq. 7. E is the heat energy released, L_{vap} is the latent heat of vaporization for water, and m is the mass that is condensed.§ L_{vap} is large, being 2,260 kJ/kg. For comparison, the latent heat of fusion is 333 kJ/kg.** Using this equation, one can compare the differences in energy requirements for condensing water as opposed to commonly practiced purification techniques.

$$(7) \quad E = L_{vap}m$$

Before using Elmer finite element analysis software, the turbulence in the system, and an order of magnitude calculation for the channel velocity at the entrance and exit was calculated using the Hagen-Poiseuille Equation (Eq. 8), the Reynolds number (Eq. 9), and the definition of volumetric flow rate (Eq. 10).††

$$(8) \quad Q = \frac{\Delta P \pi R^4}{8 \mu L}$$

* Urieli, Israe. "Specific Heat Capacities of Air." Ohio University. Linear interpolation, rounding to the nearest whole number was used to determine the specific heat at constant volume.

† If a fluid is incompressible, this means the density of the fluid is constant, meaning that if the fluid is flowing, it must be pressure driven. Air is assumed in this case to be incompressible as the temperature and pressure dependence of air density is minimal within the operating conditions.

‡ Schroeder, Daniel V. A constant volume and number of particles is assumed. The efficiency in this case can never be 1 as this assumes that pressure be zero, which would mean the system operates in a vacuum, or that $\Delta P \rightarrow \infty$. Both cases are impossible to achieve the desired result of condensing water.

§ Schroeder, Daniel V.

** Datt, Prem.

†† Bird, R. Byron, Warren E. Stewart, and Edwin N. Lightfoot.

The Hagen-Poiseuille Equation is valid for a long tube, but if it is only evaluated at the ends of the system, that is on each end, the equation gives a good approximation. In Eq. 8, Q is the volumetric flow rate, R is the radius, L is the length of the channel and μ is the viscosity.

$$(9) \quad \text{Re} = \frac{\bar{v}H}{\nu}$$

The Reynold's number is a dimensionless group, defined by Eq. 9, that is used as an indicator to how turbulent the fluid flow is within a system. The higher the Reynolds number is, the more turbulence one expects in a system. A Reynolds number of around 2000 is the transition region where a system can no longer be treated as laminar flow, and turbulent eddies must be accounted for. To determine this number, \bar{v} is the average flow velocity through the channel, H is a characteristic length-scale (such as the smallest tube diameter), and ν is the kinematic viscosity.

$$(10) \quad Q = \bar{v}A$$

In this equation, A is the cross-sectional area through which the fluid is passing. By using Eq. 8 and Eq. 10, one can solve for the average flow velocity, giving Eq. 11.

$$(11) \quad \bar{v} = \frac{\Delta P \pi R^4}{8\mu AL}$$

Because the system is 2-D, the Hagen-Poiseuille Equation is not completely accurate; the system's velocity field will be distributed quite differently from a tube. However, the order of magnitude of each will be the same. The radius is the same as the system's height, 5 mm. An analogous cross-sectional area is to treat the system as though it is as wide as tall, giving 100 mm². The length of the channel is 17 cm total. All other quantities are known for air, which has been discussed earlier.

From this, one can then calculate Reynolds numbers for each tube length used. The characteristic length scale for the systems will be the diameter of the center tube. The Reynolds numbers of the each system are all large enough to expect turbulence, of order 10⁵-10⁶. Because of this, the Reynolds-Averaged Navier-Stokes Equation, Eq. 12, was used instead of the standard Navier-Stokes Equation to provide a solution.

$$(12) \quad \rho \frac{D}{Dt} \bar{\mathbf{v}} = -\nabla \bar{p} - [\nabla \cdot \rho \bar{\mathbf{v}} \bar{\mathbf{v}}] - [\nabla \cdot (\bar{\tau}^{(v)} + \bar{\tau}^{(t)})] + \rho \mathbf{g}^*$$

The Reynolds-Averaged Navier-Stokes Equation is the Navier-Stokes Equation with the underlying assumption that the fluid flow velocity can be broken into two quantities, $\bar{\mathbf{v}}$ and \mathbf{v}' , where $\bar{\mathbf{v}}$ is the time-smoothed fluid velocity over a time interval in which \mathbf{v}' , the turbulent fluid velocity, averages to zero. The turbulent fluid velocity is associated with the fluid velocity due to eddies that form in the system, which does not carry material through the system, but rather

* $\bar{\tau}^{(t)}$ represents the turbulent momentum flux tensor, whose components can be defined by $\bar{\tau}_{ii}^{(t)} = \rho \overline{v_i' v_i'}$ and $\bar{\tau}_{ij}^{(t)} = \rho \overline{v_i' v_j'}$, the Reynolds stresses. $\bar{\tau}^{(v)}$ represents the time-smoothed viscous momentum flux, whose components can be defined by $\bar{\tau}_{ii}^{(v)} = -2\mu \frac{\partial \bar{v}_i}{\partial x_i}$ and $\bar{\tau}_{ij}^{(v)} = -\mu \left(\frac{\partial \bar{v}_i}{\partial x_j} + \frac{\partial \bar{v}_j}{\partial x_i} \right)$.

creates chaotic swirls, which do not translate fluid down the channel. Because the swirls can be thought of as closed loops, the average velocity within each average to zero over a time span T , where T represents the time it takes to pass through a full loop.*

There are various ways to solve the Reynolds-Averaged Navier-Stokes Equation computationally, however, this system was studied using the k-epsilon model. The k-epsilon model is an improvement on the mixing length turbulence model, which uses the Boussinesq Eddy Viscosity Assumption to model fluids.† This supposition states that energy that is lost to eddy circulation is analogous to the momentum lost due to random particle motion. Therefore, just as momentum loss is macroscopically proportional to the molecular viscosity, the energy lost due to eddies is proportional to the eddy viscosity.

The underlying assumptions of the k-epsilon model are the “Law of The Wall” first postulated by Theodore Von Kármán, and that turbulent viscosity is taken to be isotropic‡. The “Law of The Wall” states that the eddy viscosity should vary proportionally to the distance from a wall. While both assumptions are not accurate throughout a fluid stream, the “Law of The Wall” is accurate out to a boundary layer, while the assumption of an isotropic turbulent viscosity is most accurate away from the wall. By utilizing both assumptions, an accurate flow shape can be achieved.

Due to convergence problems, even utilizing the k-epsilon model, using the average velocity that was calculated by the Hagen-Poiseuille equation, each system was kept at a constant Reynolds number, rather than use the velocity that would be predicted from the difference in pressure required to satisfy the dew point temperature. A Reynolds number of 10^4 was selected for each system. This was used so that each system experienced turbulence, but not so much as to create severe convergence issues in solving the coinciding pressure profile.

When analyzing data, five cross-sections of the pressure distributions of each system were taken. The cross-sections were used to compare the center pressure along the length of the channel, and the pressure at four different lengths along the channel. The centerline was used for comparing total pressure differences along the system to minimize the influence that artifacts had on analysis. Artifacts in the pressure gradients mostly occurred near the edges, tending to favor the entrance and exits of the systems.

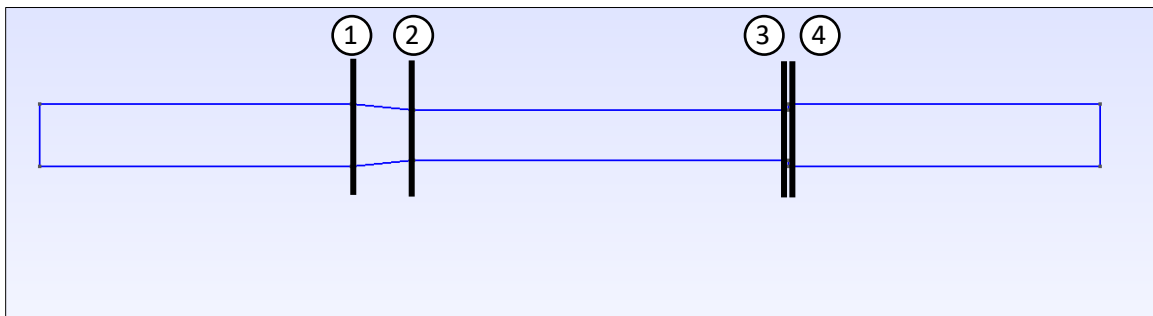


Figure 1.2 The locations of the four cross-sectional areas that were taken of the pressure distributions across the channel width. (1) Taken 5 cm along the channel, just before the system begins to constrict. (2) Taken 6 cm along the channel, at the end of constriction. (3) Taken 11.99 cm along the channel, just before sudden dilation. (4) Taken 12.01 cm, just after sudden dilation.

* Bird, R. Byron, Warren E. Stewart, and Edwin N. Lightfoot.

† Schmitt, François G.

‡ United States of America. National Aeronautics and Space Administration

Section 2. Results

For the required pressure difference to reach dew point, 1872 Pa, the Hagen-Poiseuille equation shows that the average initial velocity decreases as the minimum diameter decreases. The Reynold's number will also decrease as the minimum cross-sectional diameter and the average velocity decrease. Using Eq. 11, it was found that the entrance velocities were incredibly high. Even the minimum velocity was over double the speed of sound.

	<u>Minimum Tube Diameter (mm)</u>	<u>Reynolds Number</u>	<u>Entrance Velocity (m/s)</u>
System A	8	7×10^6	14000
System B	6	3×10^6	7800
System C	4	8×10^5	3500
System D	2	1×10^5	870

The difference along the pressure profiles of each system increased dramatically with fixed Reynolds numbers of 10^4 . As the minimum diameter decreased, the pressure difference increased. The lowest pressure difference across the centerline was approximately 130 Pa in System A, while the highest pressure difference was approximately 1100 Pa in System D. Furthermore, each pressure profile had different shapes. The pressure was lowest in different

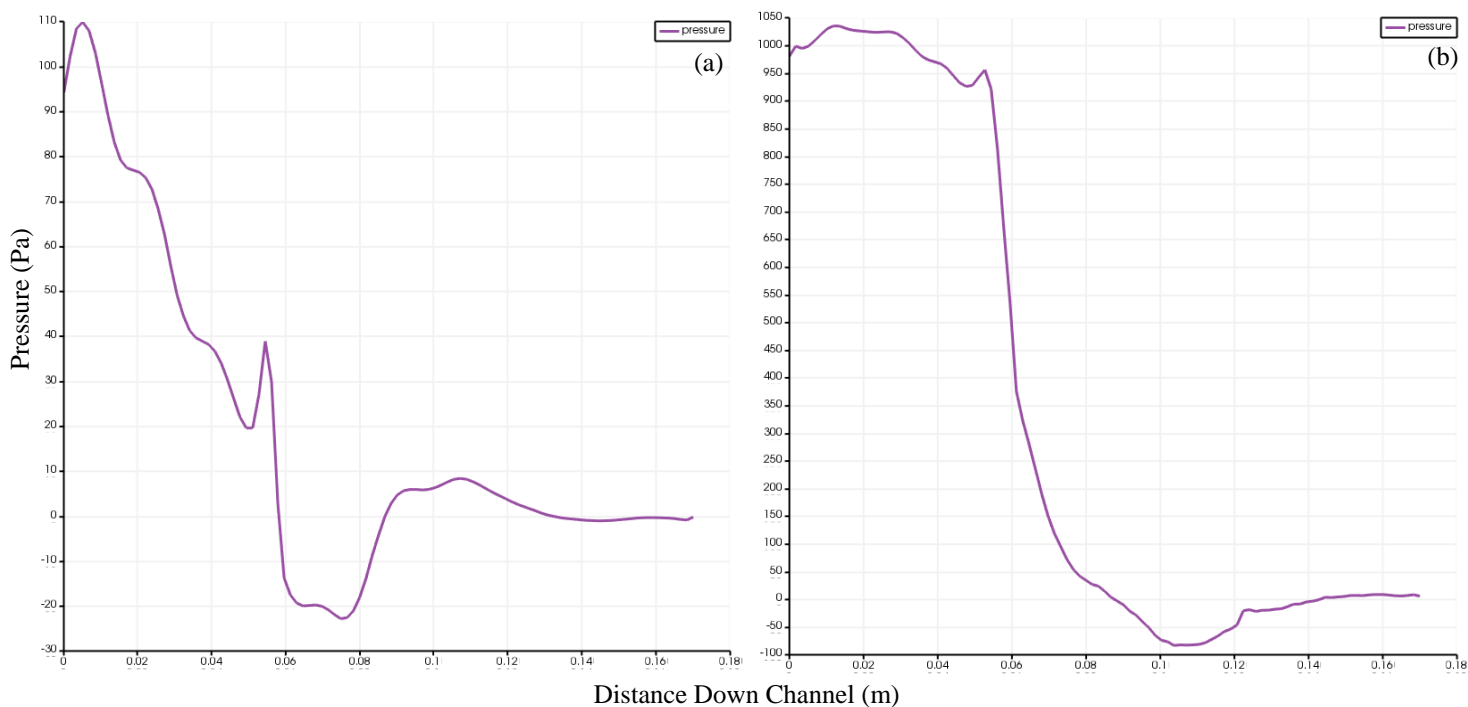


Figure 2.1 (a) Pressure difference along centerline of System A. (b) Pressure difference along centerline of System D

areas of the system. For Systems A and B, the pressure was lowest at the end of constriction, while for system C, the pressure was lowest after dilation, and for System D, the pressure was lowest just before dilation. This is directly related to the position of highest velocity, which has a response to the shape of each system.

As the minimum tube diameter decreased, the position of the highest velocity moved forward along the channel. The boundary layer of slower moving fluid near the walls within the minimum diameter region for Systems A and B were much smaller in comparison to the cross-sectional area, which meant the velocity field quickly took shape to form a blunt-nosed parabolic shape that is seen in turbulent systems. However, for Systems C and D, the size of the cross-sectional area in the minimum diameter region was much smaller in comparison to the boundary layer near the walls. In both Systems C & D, this lead to a drift in the position of the maximum velocity down the channel. At this point, the blunt-nosed parabolic shape has formed.

It is of note that Systems C and D both show signs of unstable flow shapes, as there are fluctuations of velocity across the cross-sectional area of the minimum diameter. This could be

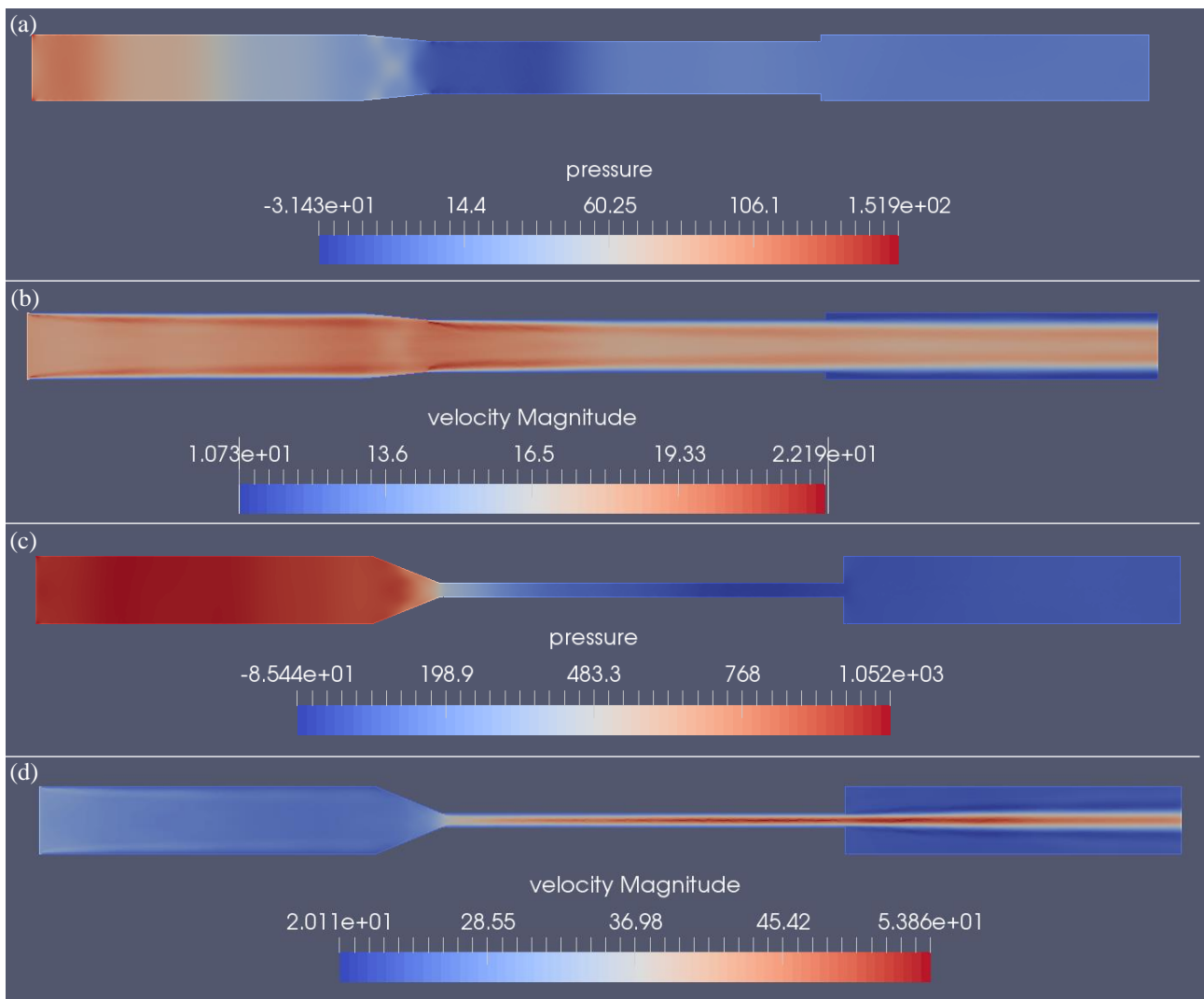


Figure 2.2 (a) System A pressure profile. (b) System A velocity profile. (c) System D pressure profile. (d) System D velocity profile.

due to the formation of eddies within that region, which could lead to an increase in temperature. This is due to the transfer of kinetic energy into thermal energy through molecular collisions within the eddies.

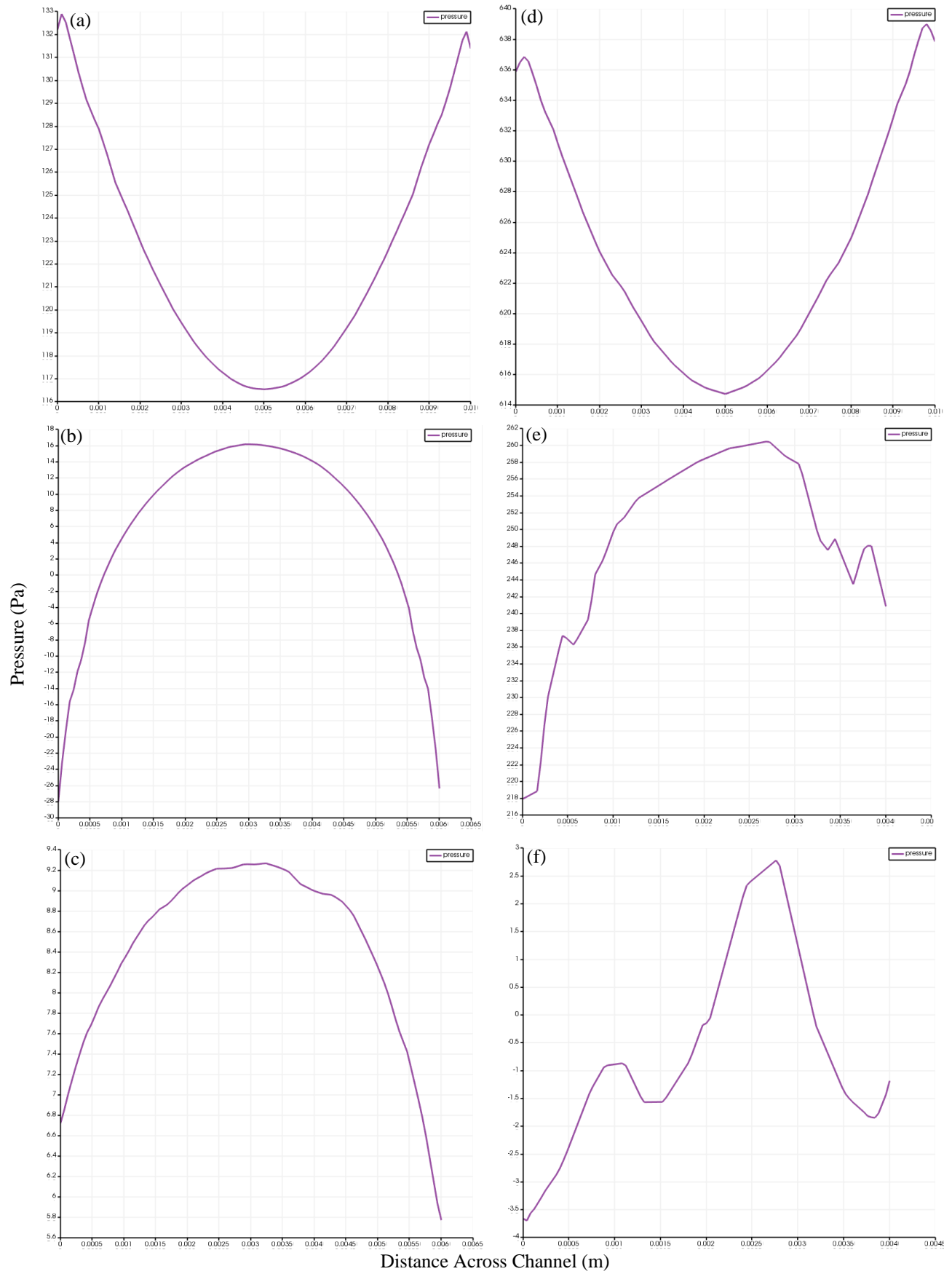


Figure 2.3 (a) System B at cross-section 1. (b) System B at cross-section 2. (c) System B at cross-section 3. (d) System C at cross-section 1. (e) System C at cross-section 2. (f) System C at cross-section 3.

Within the cross-sectional areas of each system, the pressure distributions were erratic for both Systems A and D especially, while System C showed some anomalous behavior. One could expect a symmetric pressure distribution with small aberrations; however, this was not true. For systems A, C, and D, all experiences deviations from symmetry during the constriction. This may be due to imperfections of, or instability within the simulations.

Section 3. Discussion

Because of the large entrance velocities required to induce the pressure difference resulting in possible water condensation, a large system is likely not possible, and not efficient. With a small enough system, the entrance velocity required could drop to a reasonable quantity; however, for this to be confirmed, an analysis of the thermal energy generated by eddies within the minimum diameter section should be conducted. As the cross-sectional area of the minimum diameter region decreases, viscous forces would transform more kinetic energy into thermal energy, thereby eliminating the possibility of water condensation.

Systems A and B seemed to be largely ineffective at creating a large difference in pressure between the entrance region and the exit region. While Systems C and D seemed to perform better, System D was the only system to achieve a pressure difference that was close to the required 1872 Pa to bring the air inside to the dew point. This was close, but even if any of the systems had achieved the necessary pressure difference to bring the air passing through to dew point, additional energy would have to be removed from the air to condense water. The latent heat of vaporization must be accounted for.

Due to the thermodynamic restraints, condensing water as a mode of purification can only be so efficient. If a completely efficient system is assumed, 2,260 kJ of energy is required for every kg of clean water produced. In comparison, the energy requirements for desalination is approximately 6.46 kJ/kg, depending on the salinity and energy recovery methods in place.* Desalination, however, also has other requirements not accounted for, such as transportation, which may increase this number greatly, depending on how far away the body of water is from the intended recipients of it. For wastewater treatment, the energy requirements vary a great deal depending on the size of the treatment facility, the pollutants being removed, and the types of processes utilized to remove pollutants. However, at best, 1,392 kJ/kg is required, and at worst, 13,919 kJ/kg.† One must account that for wastewater treatment, there are more biological products and solids removed than in desalination.

When comparing the energy requirements of the three techniques listed in the previous paragraph, one finds that condensing water vapor for consumption consumes much more energy than desalination, and depending on how many pollutants are removed, can be less energy efficient than wastewater treatment.

* "Seawater Desalination Power Consumption." (2011) This assumes the density of water to be 1,000kg/m³, which depending on the salinity of the water, is not always true.

† "Energy Use in Wastewater Treatment Plants ." *New Mexico Energy, Minerals and Natural Resources Department.*

Section 4. Conclusion

Condensation techniques may be used in the future to provide potable water to those in areas where standard water purification techniques may not be used; however, the energy demands of condensing water vapor are costly. Therefore, naturally occurring phenomena must be explored instead to produce water, such as the constant temperature at the bottom of bore holes in wells. However, many preexisting techniques, such as wells, are easily contaminated in areas of poor sanitation.

So, while there may be promising avenues for the exploration of new techniques to provide clean, potable water, proper sanitation is just as, if not more important to the health and well-being of a population. Engineers and scientists should look for ways to improve current methods of providing suitable water for consumption so that these water sources are not contaminated as easily.

Section 5. Acknowledgements

I would like to thank the chair of the honors committee, Dr. Joseph D. Kirtland, for allowing me to explore different creative avenues in researching the information within this document and for putting up with the multiple topic changes that it underwent. I would also like to thank the members of the committee, Dr. John D'Angelo and Roger J. Loucks, both of which have been helpful in every way possible. A special thanks to Dr. Malin Faulkenmark of the Stockholm Resilience Centre for the use of Figure 0.2 and her support of this project. Many thanks to the United States National Oceanic and Atmospheric Administration for not only compiling and processing so much meteorological data across the globe, but also for making it easily accessible. The Alfred University Honors Program was also a driving force behind the creation of this thesis as it motivated me to press on even when it seemed this project was in despair.

Section 6. References

"2013 State of the Climate: Humidity." Climate.gov. National Oceanic and Atmospheric Association, 12 July 2014. Web. 15 May 2017.

Bird, R. Byron, Warren E. Stewart, and Edwin N. Lightfoot. "Shell Momentum Balances and Velocity Distributions in Laminar Flow." *Transport Phenomena*. 2nd ed. New York: John Wiley & Sons, Inc., 2007. 45-51, 152-177. Print.

"Climate United States." U.S. Climate Data. N.p., 2017. Web. 3 Apr. 2017.

"Comparative Climatic Data." National Climatic Data Center. National Oceanic and Atmospheric Association, n.d. Web. 3 Apr. 2017.

Datt, Prem. "Latent Heat of Vaporization/Condensation." *Encyclopedia of Snow, Ice and Glaciers*. Ed. Vijay P. Singh, Pratap Singh, and Umesh K. Haritashya. N.p.: n.p., n.d. 703. Springer Netherlands, 2011. Web. 27 Mar. 2017.

"Energy Use in Wastewater Treatment Plants ." New Mexico Energy, Minerals and Natural Resources Department. Energy Star, Jan. 2015. Web. 5 Apr. 2017.

Falkenmark, Malin, Jan Lundqvist, and Carl Widstrand. "Macro-Scale Water Scarcity Requires Micro-Scale Approaches." *Natural Resources Forum* 13.4 (1989): 258-67. Web. 18 Oct. 2017.

Falkenmark, Malin, and Carl Widstrand. "Population and Water Resources: A Delicate Balance." *Population Bulletin* (1992): n. pag. Proquest Central. Web. 23 Sept. 2016.

"Global Climate Report - Annual 2016." NOAA National Centers for Environmental Information, Jan. 2016. Web. 09 Apr. 2017.

J. Schewe, J. Heinke, D. Gerten, I. Haddeland, N.W. Arnell, D.B. Clark, R. Dankers, S. Eisner, B.M. Fekete, F.J. Colón-González, S.N. Gosling, H. Kim, X. Liu, Y. Masaki, F.T. Portmann, Y. Satoh, T. Stacke, Q. Tang, Y. Wada, D. Wisser, T. Albrecht, K. Frieler, F. Piontek, L. Warszawski, and P. Kabat. "Multimodel assessment of water scarcity under climate change." Ed. Hans Joachim Schellnhuber. *Proceedings of the National Academy of Sciences* 111.9 (2014): 3245-250. Web. 4 Mar. 2014.

Kumpel, Emily, Rachel Peletz, Mateyo Bonham, Annette Fay, Alicea Cock-Esteb, and Ranjiv Khush. "When Are Mobile Phones Useful for Water Quality Data Collection? An Analysis of Data Flows and ICT Applications among Regulated Monitoring Institutions in Sub-Saharan Africa." *International Journal of Environmental Research and Public Health* 12.9 (2015): 10846-0860. Web. 22 Nov. 2016.

Kummu, M., J. H. A. Guillaume, H. De Moel, S. Eisner, M. Flörke, M. Porkka, S. Siebert, T. I. E. Veldkamp, and P. J. Ward. "The World's Road to Water Scarcity: Shortage and Stress in the 20th Century and Pathways Towards Sustainability." *Scientific Reports* 6.1 (2016): 1-16. Web. 23 Mar. 2017.

Lawrence, Mark G. "The Relationship between Relative Humidity and the Dewpoint Temperature in Moist Air: A Simple Conversion and Applications." *Bulletin of the American Meteorological Society* 86.2 (2005): 225-33. Web. 17 Mar. 2017.

"North American Surface Analyses." Weather Prediction Center. National Oceanic and Atmospheric Association, 5 Aug. 2015. Web. 4 Apr. 2017.

Schroeder, Daniel V. *An Introduction to Thermal Physics*. 1st ed. San Francisco, Calif.: Addison Wesley Longman, 2000. Print.

Schmitt, François G. "About Boussinesq's turbulent viscosity hypothesis: historical remarks and a direct evaluation of its validity." *Comptes Rendus Mécanique* 10th ser. 335.9 (2007): 617-27. HAL. Web. 24 Mar. 2017.

"Seawater Desalination Power Consumption." (2011): n. pag. WateReuse. Nov. 2011. Web. 4 Apr. 2017.

United Nations. UN Water. Investing in Water and Sanitation: Increasing Access, Reducing Inequalities UN-Water Global Analysis and Assessment of Sanitation and Drinking-Water GLAAS 2014 Report. By Didier Allély et. Al. , 2014. Print.

United States of America. National Aeronautics and Space Administration. Mechanical Similitude and Turbulence. By Theodore Von Kármán. Washington, D.C.: National Advisory Committee for Aeronautics, 1931. NASA Technical Reports Server. Web. 16 Mar. 2017.

Urieli, Israe. "Specific Heat Capacities of Air." Ohio University. Ohio University Mechanical Engineering, n.d. Web. 2 Apr. 2017.

World Health Organization. Guidelines for drinking-water quality. Geneva: World Health Organization, 2008. n.d. Web. 3 Oct 2016.